High-precision grinding for large-aperture aspherical surface based on medium-low frequency error suppression method

Guoyan Sun[1,2], Xiabin Ji[1#], Jiaoteng Ding[1], Hang Cheng[1], and Jigong Zhang[1]

1 Xi'an Institute of Optics and Precision Mechanics, Chinese Academy of Sciences, NO.17 Xinxi St., Xi'an, 710119, PR China
2 College of Artificial Intelligence, National University of Defense Technology, NO.109 Deya St., Changsha, 410003, PR China
Corresponding Author / Email: jixiabin@opt.ac.cn, TEL: +86-137-9762-9653

KEYWORDS: High-precision grinding, Large-aperture aspherical surface, Middle frequency error, Low frequency error

As a pre-processing method for large-aperture aspherical optical components (LAAOC), high-precision grinding can remove the hard-brittle optical materials with high efficiency. However, the medium-low frequency error of the ground surface induced by the high-precision grinding can seriously increase the subsequent polishing cycles and increase the manufacturing costs of LAAOC. Therefore, in this paper, high-precision grinding experiments were conducted to investigate the suppression method of medium-low frequency error. Firstly, the influence law on the medium-low frequency error of the ground surface for four main influence factors have been investigated with the synthetic optimization of these factors, in terms of the relative position error between the workpiece and grinding wheel, the radius error of the grinding wheel, grinding path planning and error compensation. Then, the kinematics analysis and homogenization optimizing of the grinding marks were studied, because grinding texture is the primary contributor of the medium-frequency error of the ground aspherical surface. In the end, the suppression method for medium-low frequency error in high-precision grinding was proposed and it was verified with grinding experiments. The results show that the suppression method proposed in this paperr can either effectively reduce the medium-frequency waviness, or greatly improve the surface figure accuracy (peak-valley value) to be within 3 μm for an off-axis aspherical mirror of 560mm diameter.

1. Introduction

With the increasing demand for high-resolution detection and imaging, the development of large aperture optical components with complex surface forms and lightweight structures has become increasingly important [1, 2]. For example, the primary mirror diameter for the European Extremely Large Telescope (E-ELT) project is 42 m, comprising 984 hexagonal sub-mirrors with a diameter of 1.45 m each. Furthermore, all sub-mirrors are off-axis aspheric surfaces made of microcrystalline glass Zerodur or optical glass ULE. The completion of all sub-mirrors is required within 4.5 years [3]. However, the large aperture and complex surface forms significantly increase processing difficulty and cycle time, posing an urgent need to expedite processing cycles and enhance efficiency for manufacturing large aperture optical components.

As a highly efficient and precise machining process [4], precision grinding plays a crucial role in the production of large-aperture optical components. However, precision grinding unavoidably introduces low-frequency grinding surface form inaccuracies and medium-frequency grinding textures. These inaccuracies and textures determine the difficulty and duration of subsequent polishing processes. Consequently, numerous studies have been conducted by scholars to investigate grinding processes for large-aperture optical components. Zhang et al. [5] processed a Φ372 mm high-steep off-axis SiC aspheric mirror using variable-axis single-point grinding, achieving a surface form accuracy (PV) of 7.8 μm after grinding. Comley et al. [6] achieved shape accuracy RMS better than 1 μm for a low-steepness Φ1450 mm caliber mirror through precision grinding. Mario et al. [7, 8] investigated the influence of grinding parameters on medium-frequency errors on machined surfaces and confirmed the correlation between medium-frequency errors and grinding texture uniformity. In this paper, precision grinding experiments were conducted on large-aperture aspherical surfaces to explore the formation mechanism, influencing factors, and suppression methods for low-frequency surface shape errors in the grinding process. This study aims to provide theoretical support for efficiently and precisely processing large-aperture optical components.

2. Design indexes for off-axis aspherical surface

The optical component was a Φ560mm off-axis aspherical surface with uniform thickness, and its mother mirror equation was as follows:

$$z(x,y)=\frac{\left(x^2+y^2\right)}{18000} \tag{1}$$

in which *x*, *y*, and *z* represent the surface form coordinates of the off-axis aspherical surface with an off-axis amount of 700 mm. The high-precision grinding of the large-aperture off-axis aspherical surface required multiple iterative processes, as shown in Fig. 1. Firstly, the mirror surface was rough ground and then precision ground. It was necessary to control and suppress the low-medium frequency error of the surface form accuracy during precision grinding.

On one hand, it required analyzing the main influencing factors of low-frequency errors and implementing certainty reduction and compensation. On the other hand, medium-frequency errors could be reduced by simulating grinding marks and homogenization regulation.

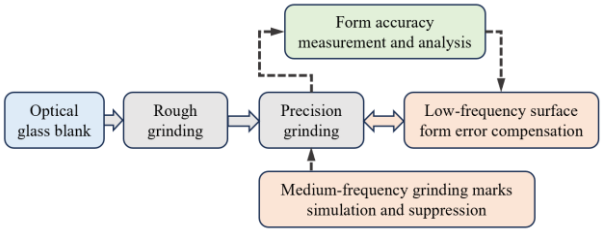

Fig. 1 Process flow of precision mirror grinding

3. Low-frequency error suppression method

3.1 Grinding motion system and grinding mode

The OptoTech MCG 500 CNC-Compact high-precision 5-ax is milling and grinding machine was adopted for the machining of the Φ560 mm off-axis aspherical optical components in this paper, as illustrated in Fig. 2. It consisted of linear motion axes in three directions, a workpiece revolving platform (C axis), a g rinding spindle, and a workpiece swing axis (A axis). The CNC linear motion axis had positioning and repeated positioning accu racies of ⩽5 μm and ±2 μm, respectively, while the position ing accuracies of the A axis and C axis were ⩽9″ and ±5″, respectively. The perpendicular grinding mode was employed.

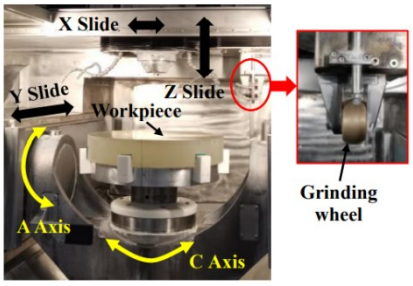

Fig. 2 Illustration of grinding machine

3.2 Grinding method and motion path

Different grinding methods and motion paths could influence grinding accuracy. For the off-axis aspherical mirror in this paper, the effects of three-axis linkage spiral grinding method, four-axis linkage spiral grinding method, and raster grinding method on surface form accuracy were compared. The grinding parameters are shown in Table 1. The surface form accuracy (PV) was 8.4 μm after Y, Z, and C-axis linkage grinding, as depicted in Fig. 3 (a); the surface form accuracy (PV) was 7.8 μm after X, Y, Z, and C-axis linkage grinding, as depicted in Fig. 3 (b); and the surface form accuracy (PV) was 5.3 μm after three-axis raster grinding, as depicted in Fig. 3 (c). Therefore, the three-axis raster grinding method achieved the highest surface form accuracy, followed by the four-axis linkage spiral grinding method.

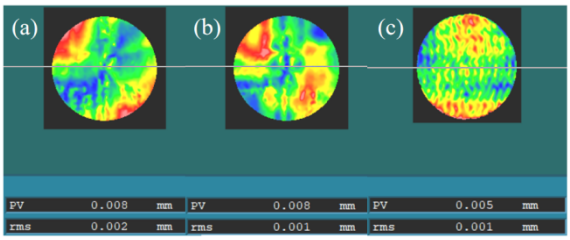

Fig. 3 The experimental results of off-axis aspherical surface form accuracy (PV): (a) three-axis spiral scanning-path, (b) four-axis spiral scanning-path, (c) three-axis raster scanning-path

Tab. 1 Grinding parameters with different scanning paths

Grinding path	Grinding depth	Feed speed	Feed Distance	Grinding wheel rotary speed
Spiral-3D	10 μm	22r/min	0.1mm	3000r/min
Spiral-4D	10 μm	22r/min	0.1mm	3000r/min
Raster-3D	10 μm	700mm/min	0.1mm	3000r/min

3.3 Zero-position error of A axis

The ideal zero-position of the A axis could ensure the perpendicularity between the gyration center of the C axis and the plane of the X and Y linear motion axes. When there was a deviation in the zero-position of the A axis, off-axis angle error would occur during the grinding of off-axis aspherical components, thus affecting surface form accuracy. Hence, based on the aspherical surface equation (1), the influence of the zero-position error of the A axis on surface form accuracy was analyzed, and the following equation was derived:

$$\begin{bmatrix} x \\ y \\ z \end{bmatrix} = \begin{bmatrix} 1 & 0 & 0 \\ 0 & \cos(\theta+\Delta\theta) & \sin(\theta+\Delta\theta) \\ 0 & -\sin(\theta+\Delta\theta) & \cos(\theta+\Delta\theta) \end{bmatrix} \begin{bmatrix} x \\ y \\ z \end{bmatrix} \tag{2}$$

where θ is off-axis angle and $\Delta\theta$ is the variation of off-axis angle error. According to the above equation, simulation analysis revealed that every time the zero-position error of the A axis changed by 0.001°, the numerical value of surface form accuracy (PV) changed by 4.9 μm. The corresponding experimental results are shown in Fig. 4 (a) and Fig. 4 (b), with PV changing by 5.6 μm.

3.4 Alignment error of Y axis

Y axis was a horizontal motion axis of workpiece feeding in the grinding process of off-axis aspherical surface and the alignment error of Y axis was a deviation between workpiece center and ideal zero-position of machine tool Y axis, which could influence off-axis amount error during the grinding of off-axis aspherical components. To simplify analysis, taking the aspherical profile curve in the meridian cross section at the two points of far and near ends as research object, assuming the ideal curvilinear equation of the cross section was $f_{id}(y)$, while the actual equation was $f_{ac}(y)$, then the surface form accuracy (PV) could be expressed as

$$e_z = f_{\mathrm{id}}(y) - f_{\mathrm{ac}}(y) \tag{3}$$

When there was an alignment error of Y axis, the following equation could be obtained

$$f_{ac}(y) = f_{id}(y + d_b \cos\theta) \tag{4}$$

where d_b is an alignment error of machine tool Y axis. When equation (4) was substituted into quation (3), the following equation could be obtained

$$e_z = f_{id}(y) - f_{id}(y + d_b \cos\theta) \tag{5}$$

According to the above equation, the analysis indicated that every time the alignment error of the Y axis changed by 10 μm, the numerical value of surface form accuracy (PV) changed by 1.1 μm. Furthermore, as the alignment error of the Y axis increased, the surface form accuracy (PV) basically exhibited a linear change within certain limits. When the alignment error of the Y axis reached 70 μm, the theoretical surface form accuracy (PV) was 7.7 μm, but the experimental value was 8.6 μm, as shown in Fig. 4 (b) and Fig. 4 (c).

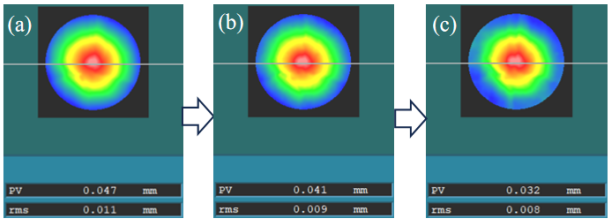

Fig. 4 Low-frequency error suppression method: (a)-(b) Effect of A-axis zero-position error on surface form accuracy (PV), (b)-(c) Effect of Y-axis alignment error 70um on surface form accuracy (PV)

3.5 Other errors

In addition, there would be an error between the true radius and the numerical radius of the grinding wheel in actual use due to installation, measurement, and abrasion, which could impact surface form accuracy. As shown in Fig. 5 (a) and Fig. 5 (b), when the radius of the grinding wheel reduced by 0.05 mm, the surface form accuracy (PV) of the off-axis aspherical surface decreased by 3 μm. Additionally, there would be an inherent error in the system under specific processing methods and conditions. To minimize this error, surface form accuracy compensation of the Z axis was employed. Accurate measurement was initially performed for the surface form accuracy after grinding, and then the feed rate was adjusted based on the residual error of the surface form, facilitating compensation machining. As illustrated in Fig. 5 (c) and Fig. 5 (d), through accuracy compensation machining of the Z axis, the surface form accuracy (PV) significantly increased from 7 μm to 3 μm, which was essentially close to the limit of the accuracy measurement capacity of a coordinate measuring machine.

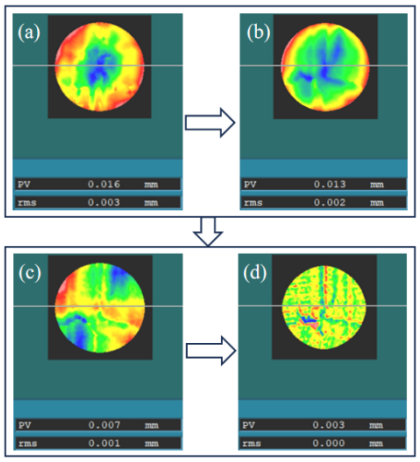

Fig. 5 Effects on surface form accuracy (PV) by: (a)-(b) Grinding wh eel radius error, (c)-(d) Surface form accuracy compensation

4. Medium -frequency error suppression method

Since there was a direct relationship between medium frequency errors and grinding marks, the suppression of medium frequency errors could be achieved by modulating the evenness of grinding marks [7, 8]. The grinding point distribution equation [9] was established for the aspherical grinding in this paper, and the simulation of grinding marks could be achieved for the aspherical surface grinding according to the equation. Based on the simulation results of grinding marks, further optimization of grinding parameters was achieved by moderately increasing the grinding wheel rotation speed, reducing the workpiece feed speed, and adjusting the workpiece rotation speed, which improved the grinding surface texture, and the evenness of grinding marks could be adjusted. As illustrated in Fig. 6, the trajectory patterns of the grinding surface could be adjusted through the optimization of grinding parameters. With the increasing density of grinding points, they formed circular spiral patterns, radial spiral patterns, and uniform patterns, as shown in Fig. 6 (a), Fig. 6 (c), and Fig. 6 (e), respectively. Correspondingly, the grinding verification test was carried out according to the simulation parameters. A white-light interferometer was adopted to observe the appearance of the grinding surface and measure surface roughness. The experiment showed that the texture pattern of the grinding surface was consistent with the simulation result. As shown in Fig. 6 (b), Fig. 6 (d), and Fig. 6 (e), the grinding surface roughness of circular spiral patterns, radial spiral patterns, and uniform patterns were 133 nm, 110 nm, and 83 nm, respectively. This suggests that the simulation optimization of grinding parameters can achieve the evenness of grinding marks and reduce surface roughness.

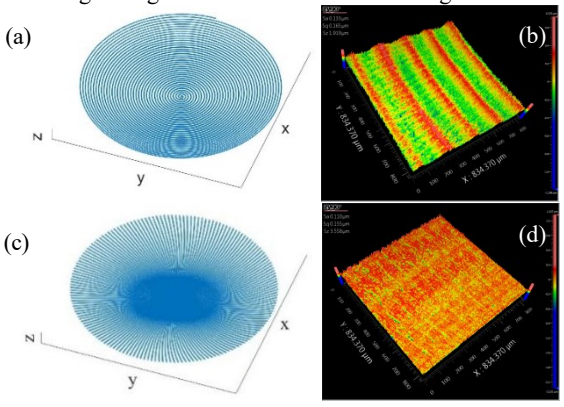

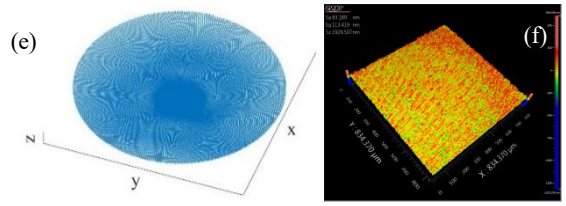

Fig. 6 The simulation results and experiment results of grinding surface marks:(a) simulation result-circular spiral pattern, (b) experiment result-circular spiral pattern, (c) simulation result-radial spiral pattern, (d) experiment result-radial spiral pattern, (e) simulation result-uniform pattern, (f) experiment result- uniform pattern

5. Conclusions

In this paper, medium-low frequency error suppression methods were investigated separately to improve the accuracy and quality of the grinding surface. The conclusions drawn are as follows:

1.The surface form accuracy of the large-aperture aspherical grinding surface can be effectively improved through the analysis of influencing factors, deterministic integrated control, and compensation. In this study, the surface form accuracy (PV) of a 560mm off-axis parabolic mirror can achieve 3 μm after grinding.

2.Through modeling, simulation, and suppression control of the grinding texture, the medium frequency error and surface roughness of the large-aperture aspherical grinding surface can be significantly reduced.

ACKNOWLEDGEMENT

This work was supported by the National Natural Science Foundation of China (NSFC) [grant number 52105493], the Natural Science Basic Research Plan in Shaanxi Province of China [grant number 2023-JC-QN-0713], the Hunan Provincial Natural Science Foundation of China [grant number 2023JJ40670], the Youth Innovation Promotion Association CAS [grant number 2023423] , and the China Postdoctoral Science Foundation [grant number 4139ZRY4].

REFERENCES

1. Graves LR, Smith GA, Dániel Apai, et al., "Precision Optics Manufacturing and Control for Next-Generation Large Telescopes," Nanomanufacturing and Metrology., Vol. 2, pp. 65-90, 2019.
2. Kim D, Choi H, Brendel T, et al., "Advances in optical engineering for future telescopes," Opto-Electronic Advances., Vol. 4, No. 6, pp. 210040-210040, 2021.
3. Stepp L M, Gilmozzi R, Hall H J, et al., "European Extremely Large Telescope: progress report," SPIE Astronomical Telescopes and Instrumentation, No. 9145E, 2014.
4. Zhang S, Guo X, Yuan S, et al. "Insight on the structural changes of glass-ceramics during nanoindentation derived from reactive force-field-based molecular dynamic simulations," Applied Surface Science., Vol. 571, No. 151375, 2022.
5. Zhang ZY, Zheng LG., "Grinding strategies for machining the off-axis aspherical reaction-bonded SiC mirror blank," Chinese Optics Letters., Vol. 12, No. 1, pp. 1-5, 2014.
6. Comley P, Morantz P, Shore P, et al., "Grinding metre scale mirror segments for the E-ELT ground based telescope," CIRP Annals., Vol. 60, No. 1, pp. 379-382, 2011.
7. Mario P, Olga K, Rainer B, et al., "Mid-spatial frequency error generation mechanisms and prevention strategies for the grinding process , " Journal of the European Optical Society-Rapid Publications., Vol. 16, No. 19, 2020.
8. Mario P, Uwe B, Rainer B, et al., "MSF-error prevention strategies for the grinding process," Proc. SPIE 11171., Sixth European Seminar on Precision Optics Manufacturing, 1117106, 2019.
9. Sun GY , Shi F , Zhang BW , et al., "Surface generation mechanism of the rotary ultrasonic vibration–assisted grinding of aspheric glass ceramics," The International J ournal of Advanced Manufacturing Technology, Vol. 124, No. 7, pp. 2579–2595, 2023.